

# Microscopic and Macroscopic States in Neural Networks

Author: Gerard Valentí Rojas

*Facultat de Física, Universitat de Barcelona, Diagonal 645, 08028 Barcelona, Spain. and  
Centre de Recerca Matemàtica, Campus de Bellaterra, Edifici C, 08193 Bellaterra, Spain.\**

Advisor: Alexander Roxin and Co-advisor: Albert Díaz-Guilera

**Abstract:** Firing patterns in neurons are thought to be key in the understanding of how the brain works. Trying to model the behaviour of neural networks is the current state-of-the-art in several scientific disciplines, but often these models are analytically intractable due to their complexity and high dimensionality. Recently, the Lorentz Ansatz proposed by Montbrió, Pazó and Roxin [1], showed that an exact description of macroscopic observables for a neural network is possible under some constraints. This thesis is aimed to re-deriving the ansatz based on the existing work of Montbrió et. al. and analyzing the different states encountered in the model using Bifurcation Theory. We also extend the ansatz and relax some of the constraints. Furthermore, we build and run some simulations of a Quadratic Integrate-and-Fire network to test the theory and its generalization.

## I. INTRODUCTION

A spike or action potential is a brief reversal in electrical polarization across the membranes of cells. Such signals are short pulses of few *ms* long, which are triggered by a stimulus and whose shape has been well characterized. It is believed [4] that not a single action potential, but the spiking patterns and their timing, can shed some light on how the coding of information in neurons is done. Up to this day, many firing modes have been found and reproduced in current neural models [5].

The spiking mechanism in a single neuron can be described by the membrane potential  $V(t)$ , defined as the inside-outside difference of electric potential in a cell. Before and after the spike, the cell is found at a stable potential  $V_{rest} \approx -65mV$ . An external electrical input can produce excitations in the membrane potential such that, when a certain value  $V_{thres}$  is exceeded, a spike is generated. When neurons fire an action potential,  $V(t)$  increases of the order of  $100mV$  and the system undergoes a refractory period in which inputs, and therefore spikes, are suppressed, so there is no overlapping between two action potentials.

Detailed neuron models such as the Hodgkin-Huxley [3] have shown incredibly accurate results for one or few neurons, being able to reproduce many firing patterns. But although we can theoretically consider a single neuron, these cells are found in nature embedded in networks of billions of elements, often in complexly connected environments. It is this large-scale behaviour what can give rise to the emergence of collective phenomena such as synchronization of states [1] or memory recalling [2].

Realistic neuron models (e.g. the Hodgkin-Huxley) have been proven computationally intractable for large-scale simulation given their complexity, and remain impractical for the study of collective phenomena. Integrate-and-Fire models showed up as a computationally efficient alternative to these complex models and can be used to study general phenomenology of neuronal dynamics. Linear Integrate-and-Fire (LIF) models are even

tractable analytically, but do not capture most of these emergent phenomena cited above. Furthermore, microscopic (single neuron) and macroscopic (collective) descriptions of neuronal systems are still not in good agreement with any of the known models.

In 2015, a novel approach [1] based on the so-called *Lorentz Ansatz* (LA) was developed considering a *Quadratic Integrate-and-Fire* (QIF) network. The QIF model lies somewhere between the over-simplicity of the LIF models and the computationally inefficient Hodgkin-Huxley-type. It was proposed that, under some constraints, the dynamics of a QIF model driven by a large number of microscopic equations, could be described using only few macroscopic coupled differential equations.

## II. THE QIF MODEL AND THE LORENTZ ANSATZ

The Quadratic Integrate-and-Fire (QIF) model is found to be a simple but realistic approach near the spiking threshold ( $V_{thres}$ ). Although it is more complex than Linear Integrate-and-Fire models, it is still computationally manageable ( $\mathcal{O}(10)$  FLOPS). It is generically defined by a set of  $N$  microscopic equations (one for each neuron) of the form  $\frac{dV}{dt} = V^2 + K$ , where  $N$  is the number of neurons of the system,  $V(t)$  is the membrane potential and  $K$  is a real positive constant. Moreover, it is exactly solvable:

$$V(t) = \sqrt{K} \tan(\sqrt{K}t + \sqrt{K}t_0) \quad (1)$$

and diverges periodically. When  $V(t \rightarrow t') \rightarrow \infty$  it is assumed that there is a spike at  $t = t'$ . Since neurons interact, these  $N$  equations have to be coupled and it is not possible to have an analytic solution any more. Nevertheless, we can think of a network topology which preserves some degree of symmetry, so the problem can still be manageable. For this reason, we assume an all-to-all (fully connected) configuration following the equation:

$$\frac{dV_j(t)}{dt} = [V_j(t)]^2 + \eta_j + J S(t) + I_{ext}(t) . \quad (2)$$

---

\* Electronic Address: gvalenti.physics@gmail.com

$V_j$  is the potential for each neuron,  $\{V_j\}_{j=1,\dots,N}$ . The values  $\eta_j$  provide heterogeneity to the network.  $J$  is the synaptic weight ([11]\*).  $I_{ext}$  is an external input current depending on time and  $S(t)$  is the synaptic activity, which couples the neurons, and is taken as  $S(t) = \frac{1}{N} \sum_{j=1}^N s_j(t)$ , where:

$$s_j(t) = \int_{t_0}^t \frac{\exp(-\frac{t-t'}{\tau_s})}{\tau_s} \sum_{\{spikes\}} \delta(t' - t_{spike}) dt'. \quad (3)$$

Since the coupling is all-to-all, each neuron contributes to the  $S(t)$  term. The result is that if some element of the network fires, the other  $N-1$  elements will notice a small change in their membrane potentials. Therefore, there must be a sum for all neurons and all the spikes fired within a time  $t$ . See in Eq. (3) that each spike is approximated as a Dirac  $\delta$ , this is not mandatory and further research has been made for more complex spike-modelling (see [8]). Hence, it is taken in this way for simplicity provided a spike is a fairly short pulse.

If there is no spike for neuron  $j$  between  $t_0$  and  $t$ ,  $s_j(t) = 0$ , while every spike produced gives a contribution  $\mathcal{O}(\frac{1}{\tau_s} \exp(-t/\tau_s))$  to  $s_j(t)$ , where  $\tau_s$  stands for the synaptic time constant. This is motivated by experimentally and historically [7]. Provided Eq. (2) diverges, we will consider a reset in  $V_j(t)$  every time a spike is triggered according to the rule  $V_j(t) \geq V_{cutoff} \implies V_j(t) \leftarrow V_{reset}$ , where  $V_{cutoff} = -V_{reset}$  is taken in the limit  $V_{cutoff} \rightarrow \infty$ .

If we take the thermodynamic limit, where  $N \rightarrow \infty$ , we can move onto a continuous formulation of the problem. In this framework, we can drop the subscripts and introduce a density function  $\rho(V|\eta, t)$  as the fraction of the neurons with a membrane potential  $V$  and a parameter  $\eta$  at a given time  $t$ . The function must satisfy the normalization condition  $1 = \int_{-\infty}^{+\infty} dV \int_{-\infty}^{+\infty} d\eta \rho(V|\eta, t)g(\eta)$  for any distribution  $g(\eta)$ . Since the number of oscillators is conserved, e.g. there are no sources nor sinks, the dynamics of the system should satisfy the 1D-continuity equation:

$$\frac{\partial \rho}{\partial t} + \frac{\partial(\rho \dot{V})}{\partial V} = 0. \quad (4)$$

Here  $\dot{V}$  is the time derivative of the membrane potential, given by Eq. (2). See that the stationary continuity equation, i.e.  $\partial_V(\rho_0 \dot{V}) = 0$ , is solvable for  $I_{ext} = const$ , with the trivial solution  $\rho_0(V|\eta) \propto [V^2 + \eta + JS + I_{ext}]^{-1}$ , which is a Lorentzian function. Montbrió, Pazó and Roxin assumed in [1] an extension of this last solution for any time. They stated that the solution of Eq. (4), independently of the initial condition, would converge to a Lorentzian-shaped function:

$$\rho(V|\eta, t) = \frac{1}{\pi} \frac{x(\eta, t)}{[V - y(\eta, t)]^2 + x(\eta, t)^2}. \quad (5)$$

This is the so-called Lorentz Ansatz (LA). Here,  $x(\eta, t)$  is the half-width (i.e. half of FWHM) of the distribution while  $y(\eta, t)$  corresponds to its center.

The validity of the LA is motivated by its convergence to an *Ott-Antonsen* (OA) manifold [6], which can be seen transforming the QIF network into theta-neurons (i.e. phase oscillators) via  $V = \tan(\theta/2)$ , finding the transformed of Eq. (2) and Eq. (5), so we obtain a  $\tilde{\rho}(\theta|\eta, t)$ .

The OA ansatz is widely accepted in neuroscience and non-linear dynamics and allows the description of the evolution of a complex order parameter in a low-dimensional subspace. In this case, the order parameter is also complex and given by  $W(t) = \int_{-\infty}^{+\infty} w(\eta, t)g(\eta) d\eta$ , where  $w \equiv x + iy$  and  $g(\eta)$  is the distribution function of the values  $\eta$ , which is usually taken as a symmetrically unimodal distribution (e.g. a Gaussian or a Lorentzian). Since it is possible to map the order parameter  $W$  to the well-known Kuramoto order parameter  $Z = Re^{i\theta}$  (ref. [9]) via biholomorphic mapping, we legitimate the use of this quantity to describe the network macroscopically.

Having justified the LA and the order parameter  $W$  we want to relate the quantities  $x(\eta, t)$  and  $y(\eta, t)$  with some observable of our ensemble of neurons. Firstly, recalling that  $y(\eta, t)$  is the mode of the Lorentzian (Eq. (5)), we can define  $y(\eta, t)$  as  $\lim_{L \rightarrow \infty} \int_{-L}^{+L} V \rho(V|\eta, t) dV$ . It is worth noting that we take the integral between  $-L$  and  $+L$  and then, make  $L$  tend to infinity. This is to avoid singularities due to the fact that the mean value of a Lorentzian is undefined.

Substituting the LA Eq. (5) into Eq. (4) we can obtain the dynamics of  $x$  and  $y$  for a given value of  $\eta$ :

$$\begin{cases} \dot{x} = 2xy & (a) \\ \dot{y} = \eta + JS(t) + I_{ext}(t) - x^2 + y^2 & (b) \end{cases}, \quad (6)$$

where the overdot denotes again a time-derivative. Combining Eq. (6a) and (6b) we can obtain the dynamics of the complex order parameter  $w(\eta, t) = x(\eta, t) + iy(\eta, t)$ . Recall for future steps that  $x$  and  $y$  still depend on  $\eta$ .

The firing rate of the ensemble can be defined as  $r(t) = \lim_{V \rightarrow +\infty} \int_{-\infty}^{+\infty} (\rho \dot{V})g(\eta) d\eta$ , where  $\rho \dot{V}$  is the density current. Using Eq. (5) and (2) and taking the limit  $V \rightarrow \infty$ , we obtain:

$$r(t) \cong \int_{-\infty}^{+\infty} \frac{x(\eta, t)}{\pi} g(\eta) d\eta, \quad (7)$$

while the mean membrane potential  $v(t)$  can be defined as:

$$v(t) = \int_{-\infty}^{+\infty} y(\eta, t)g(\eta) d\eta. \quad (8)$$

Now, the firing rate  $r(t)$  and the mean membrane potential  $v(t)$  are two macroscopic observables of the neural network, but the activation  $S(t)$  is still unrelated. This can be solved by observing that  $S(t)$  tends to  $r(t)$  as  $\tau_s \rightarrow 0$  or, in other words, considering that synapses take place in very short time lapses.

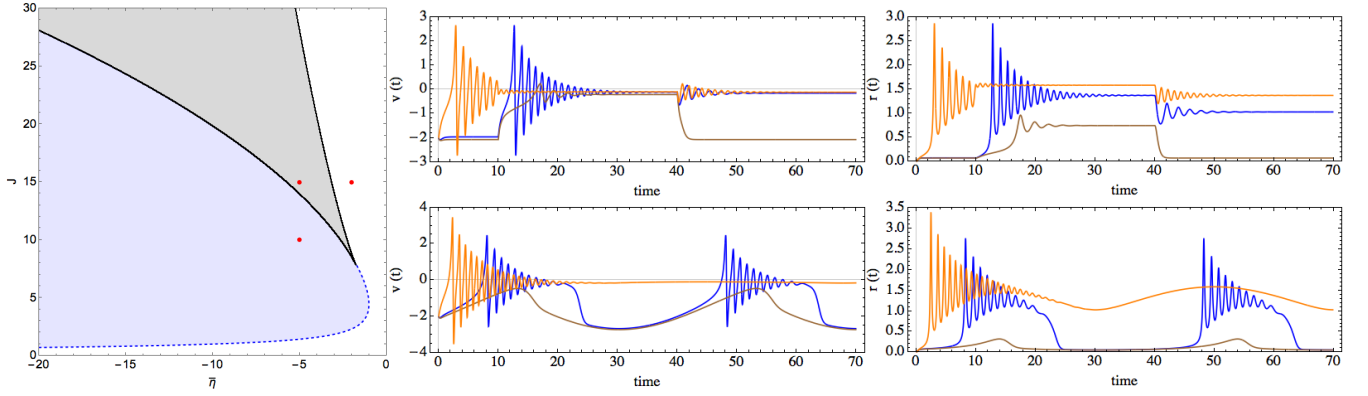


Figure 1. Phase diagram for the LA model and the macroscopic observables  $r(t)$  and  $v(t)$  obtained with the FREs (Eq. (9)). (Left) Phase diagram of the system in the  $(\bar{\eta}, J)$  phase space. It is worth noting that we can rescale the system variables dividing Eq. (9) by  $\Delta$  so the analysis can be made in terms of  $\bar{\eta}^* = \bar{\eta}/\Delta \rightarrow \bar{\eta}$  and  $J^* = J/\sqrt{\Delta} \rightarrow J$ . We distinguish three phases whose boundaries are given by the Real-Complex eigenvalue boundary (dashed-blue) and the Saddle-Node bifurcation (solid-black). The macroscopic observables are studied in each phase (three red dots). The mean membrane potential  $v(t)$  (center) and rate  $r(t)$  (right) over time are shown. The external input is taken as a step current ( $I_0 = 3$  for  $10 < t < 40$  and 0 otherwise) for the top panels while a sinusoidal forcing ( $I_0 \sin(\omega t)$ ,  $I_0 = 3$ ,  $\omega = \pi/20$ ) is taken for the ones at the bottom. (Center, Right panels) The blue line shows the behaviour in the bistable regime (grey area) at  $(\bar{\eta}, J) = (-5, 15)$ , the brown line corresponds to the stable node region (blue area) at  $(\bar{\eta}, J) = (-5, 10)$  and the orange one corresponds to the stable focus region (white area) at  $(\bar{\eta}, J) = (-2, 15)$ .

In order to use Eq. (7) and (8) to get the dynamics of the observables, we first have to consider the distribution  $g(\eta)$  that provides heterogeneity to the network. In the following, we will assume that neurons are Lorentzian distributed with center  $\bar{\eta}$  and half-width  $\Delta$ . Although taking this distribution is not strictly necessary, it is assumed in [1, 6] for simplicity and for the reduction of dimensionality of the problem it offers. See that this Lorentzian has two poles located at  $\eta = \bar{\eta} - i\Delta$  and  $\eta = \bar{\eta} + i\Delta$ , so we can use Cauchy's Residue Theorem ([12]\*\*\*) to integrate Eq. (7) and (8). Closing a semicircular integration contour around the pole  $\eta = \bar{\eta} - i\Delta$ , we obtain the solutions  $r(t) = \frac{1}{\pi} x(\eta = \bar{\eta} - i\Delta, t)$  and  $v(t) = y(\eta = \bar{\eta} - i\Delta, t)$  respectively for Eq. (7) and (8). This allows us to redefine the order parameter in terms of  $r(t)$  and  $v(t)$  as  $w(t) = \pi r(t) + i v(t)$ . Rewriting Eq. (6a) and (6b) using the macroscopic observables, we get:

$$\begin{cases} \dot{r} = 2rv + \frac{\Delta}{\pi} & (a) \\ \dot{v} = v^2 + \bar{\eta} + Jr(t) + I_{ext}(t) - (\pi r)^2 & (b) \end{cases} \quad (9)$$

These are the so-called *Firing Rate Equations* (FREs), one of the major achievements by Montbrío, Pazó and Roxin in [1]. The FREs provide a mean field description of the dynamics of the network, i.e. they are the macroscopic equations that drive the system. See that this description holds in the thermodynamic limit, for a fully-connected scheme, with a quenched heterogeneity ( $\eta$ ) Lorentzian distributed, considering fast synapses and taking spikes as  $\delta$ -functions. In the following, we will show that even though this model is developed for a particular simplified system, it captures quite complex behaviours. Notice also that these coupled equations are nonlinear, so numerical integration is required to solve them.

### III. PHASE DIAGRAM ANALYSIS

The construction of a phase diagram can provide an intuitive idea of how the system, described by the FREs, should behave. In order to do so, we study the parameters  $\bar{\eta}$ ,  $\Delta$  and  $J$  that fully determine the system if we consider no external forcing, i.e.  $I_{ext}(t) = 0$ . As Linear Stability Theory dictates, we set  $\dot{r} = \dot{v} = 0$  in Eq. (9) to study their fixed points. Solving these equations is quite tedious, but nonetheless, we can qualitatively analyse the number and type of solutions and use the Jacobian Matrix ( $\mathcal{J}$ ) to study the bifurcations we encounter. The system of equations  $\dot{r} = \dot{v} = 0$  has four fixed points, three of them physical. Evaluating the Jacobian  $\mathcal{J}$  for each of the physical fixed points, we find a saddle, a stable node and a stable focus according to their eigenvalues.

A Saddle-Node bifurcation can be found when  $\det[\mathcal{J}(r_0, v_0)] = 0$ , where  $(r_0, v_0)$  denotes a fixed point. Substituting  $v_0(r_0)$  obtained taking  $\dot{r} = 0$  in Eq. (9a), we can find  $J_{SN}(r_0)$ . If we now plug it in Eq. (9b) where we impose  $\dot{v} = 0$ , we get the value of  $\bar{\eta}_{SN}(r_0)$

$$\begin{cases} \bar{\eta}_{SN} = -\frac{3\Delta^2}{(2\pi r)^2} - (\pi r)^2 & (a) \\ \bar{J}_{SN} = \frac{\Delta^2}{2\pi^2 r^3} + 2\pi^2 r & (b) \end{cases} \quad (10)$$

Determining the expression for the eigenvalues ( $\lambda = -(\Delta/2\pi^2 r_0) \pm \sqrt{2r_0(J - 2\pi^2 r_0)}$ ), one can also find the curve that separates real eigenvalues ( $-\alpha \pm \beta$  type) from complex ones ( $-\alpha \pm i\beta$  type) by imposing  $J = 2\pi^2 r_0$ . Hence, we obtain:

$$\begin{cases} \bar{\eta}_{RC} = -\frac{4\pi^4 r^4 + \Delta}{(2\pi r)^2} & (a) \\ \bar{J}_{RC} = 2\pi^2 r & (b) \end{cases} \quad (11)$$

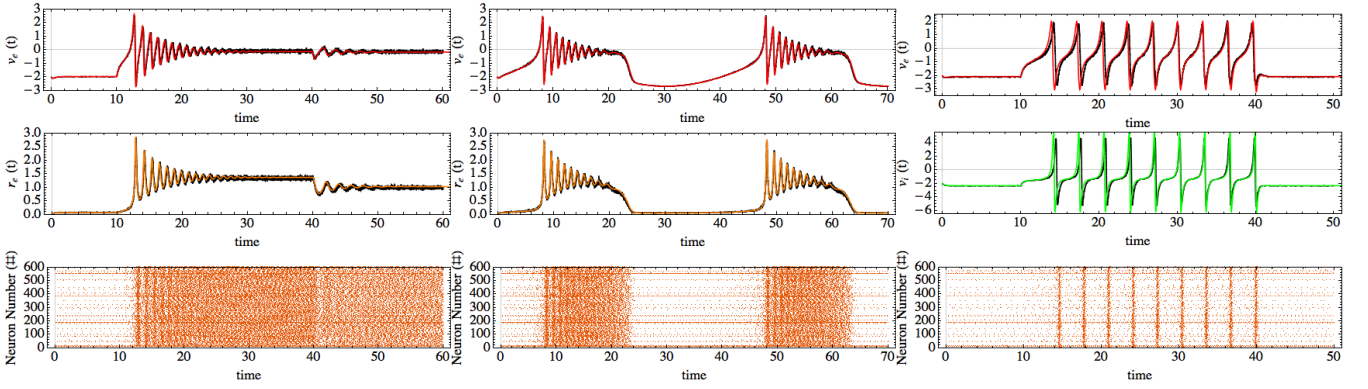


Figure 2. Mean membrane potential  $v(t)$ , firing rate  $r(t)$  and raster plots in the extended LA. Numerical simulations (black lines) are compared to FRES (coloured lines). Parameters for the external inputs are taken in a similar fashion to Figure (1). (Left, Center) These panels show the dynamics of an excitatory population with a step input current and a periodic forcing, respectively. The network is placed at the bistability region  $(\bar{\eta}_e, J_{ee}, J_{ie}) = (-5, 15, 0)$  and there is only excitatory-excitatory interaction. (Right) This panel shows the mean potential for excitatory (red) and inhibitory (green) neurons for  $(J_{ee}, J_{ie}, J_{ei}, J_{ii}) = (15, 5, 10, 15)$  with a step input current. At the bottom, the raster plots depict if a spike is fired (dot) or not (blank space) over time for the first 600 neurons. Notice that synchronization appears in the raster plots (i.e. vertical lines) when the forcing is applied or removed. In the right panel, inhibition prevents the system from transiting, even though the forcing is persistent.

Taking into account this analysis, we obtain the phase diagram of Figure (1), in which we can distinguish three regimes. The blue area in Figure (1, left panel) corresponds to a low activity phase, where there is a stable node. The white area corresponds to a high-activity phase, where a stable focus is located. Finally, the grey area stands for a bistable regime where the system tends to flow to any of the other two stable fixed points. The presence of a stable focus is quite groundbreaking, since the transition of the system from the bistability region to the highly active regime is achieved via damped oscillations. These are mean field oscillations that account for the presence of a synchronization on the firing of action potentials during the flow to a stable fixed point. Synchronization plays an important role in many different contexts including physics, biology or sociology [10], so the study of this transition can shed some light into how synchronous states appear in nature. In the center and right panels of Figure (1) we have represented the solutions of the FRES (Eq. (9)) for three points near the phase boundary, so we get an intuitive idea of the onset of these damped oscillations. We find that, when the system is located at the bistable region (blue line, center and right panels of Figure (1)) the damped oscillations are induced by the external forcing. For a sustained input, the system is able to transit to the high-activity phase, while for the periodic input the network returns to a low-activity stage after each burst period. It is worth noting that when the system is initially in the high-activity region (orange line, center and right panels of Figure (1)) the damped oscillations are intrinsically triggered in the network. The sustained external forcing therefore, only assists for a faster convergence while the oscillating input does not perturb enough the network to cause excitations.

See that in the context of globally coupled oscillators, this process can be thought as the transition from an asynchronous state to a (at least partially) synchronous

state, as it is the case for the Kuramoto oscillators [9, 10].

#### IV. MODEL EXTENSIONS

The model discussed up to this moment describes a population of excitatory ( $e$ ) neurons, which produces a positive change in the membrane potential when a spike is triggered. In real biological networks, we can encounter a second type of neurons, known as inhibitory ( $i$ ), which produce a negative post-synaptic potential. Both populations can be implemented taking into account all the possible synapses (e.g.  $e \leftrightarrow e, i \leftrightarrow e, i \leftrightarrow i, e \leftrightarrow i$ ). The microscopic description of such a system is analogous to the model for only excitatory neurons (Eq. (2)), except for the consideration of the four types of coupling between elements  $(J_{ee}, J_{ei}, J_{ie}, J_{ii})$ . Therefore, we obtain the evolution for the two populations of neurons:

$$\begin{cases} \dot{V}_j^{(e)} = [V_j^{(e)}]^2 + \eta_j^{(e)} + J_{ee}S_e - J_{ie}S_i + I_{ext}^{(e)} & (a) \\ \dot{V}_j^{(i)} = [V_j^{(i)}]^2 + \eta_j^{(i)} + J_{ei}S_e - J_{ii}S_i + I_{ext}^{(i)} & (b) \end{cases} \quad (12)$$

In the derivation of the FRES, Montbrió et. al. considered a constant synaptic weight ( $J$ ), we can relax this constraint considering a continuous distribution of these couplings in the same way it was done for  $\eta$ . Hence, we can consider new Lorentzian distributions that set the values of  $J_{\alpha\beta}$ .

Taking into account these extensions, we can obtain a new set of (generalized) FRES of the form:

$$\begin{cases} \dot{r}_e = 2r_e v_e + \frac{\Delta_e}{\pi} + \Gamma_{ee} \frac{r_e}{\pi} + \Gamma_{ie} \frac{r_i}{\pi} & (a1) \\ \dot{v}_e = v_e^2 + \bar{\eta}_e + J_{ee} r_e - J_{ie} r_i + I_{ext}^{(e)} - (\pi r_e)^2 & (b1) \\ \dot{r}_i = 2r_i v_i + \frac{\Delta_i}{\pi} + \Gamma_{ei} \frac{r_e}{\pi} + \Gamma_{ii} \frac{r_i}{\pi} & (a2) \\ \dot{v}_i = v_i^2 + \bar{\eta}_i + J_{ei} r_e - J_{ii} r_i + I_{ext}^{(i)} - (\pi r_i)^2 & (b2) \end{cases} \quad (13)$$

where  $(\Gamma_{ee}, \Gamma_{ie}, \Gamma_{ei}, \Gamma_{ii})$  are the respective half-width of the mutually independent Lorentzian distributions for the four synaptic weights.

## V. NUMERICAL SIMULATIONS

We build an all-to-all connected QIF model using the extended microscopic equations (Eq. (12)) for  $N$  neurons, taking  $N$  large enough to satisfy the thermodynamic limit. The synaptic activity  $S_{e,i}(t)$  is evaluated using its derivative formulation  $\tau_s \dot{S}_{e,i} = -S_{e,i}(t)$ , and run in parallel to Eq. (12). This implementation shares some common threats with the Izhikevich version of the QIF model [5], proven to be much more realistic than a plain QIF.

In the limit of  $J_{ie} \rightarrow 0$  and  $J_{ee} \rightarrow \Gamma_{ee}$ , we expect, for the excitatory population, to recover the results shown in Figure (1). In Figure (2 left and right), we observe how the extended FREs (coloured lines) reproduce the simulated behaviour of the network (in black). Furthermore, notice that we find the results of Figure (1) for the bistable point ( $\bar{\eta} = -5, J = 15$ ). This clearly shows that Eq. (13) converge to Eq. (9) in the correct limit, and that the FREs can capture the dynamics of the network.

Moreover, in Figure (2 bottom left/center) we observe synchronization, i.e. most neurons spiking at the same time. This is seen when vertical lines appear in the raster plots. As the oscillations are damped, so is the synchronization, so it is only a transitory state.

We further show the potential of the extended FREs and simulations in Figure (2 right), where we consider  $J_{ei}, J_{ie} \neq 0$ , so we allow the interaction between populations. It is worth noting how the periods of synchronization appear for excitatory and inhibitory populations, but even though the input is the same as in the last case, the system falls back to the low activity state.

## VI. CONCLUSIONS

The Lorentz Ansatz is re-derived for a Quadratic Integrate-and-Fire network, based on the previous work of Montbrió et. al. [1]. A set of Firing Rate Equations

(Eq. (9)) is found to describe the mean dynamics of the network. The evolution of the macroscopic observables  $r(t)$  and  $v(t)$  shows that the system can be found at a bistable regime. In this scenario, if an external forcing is applied (e.g. in the form of an electrical current), the network undergoes a period of highly fluctuating activity, which ends differently depending on the duration of the input. A persistent input is shown to perturb the system enough to transit to a high activity phase (Figure (2 left)), even though the forcing is removed afterwards. An oscillatory input is proven not enough to force this phase transition, so every time the forcing ceases, the system falls back to a low activity phase (Figure (2 center)). As already pointed out J. J. Hopfield [2], these transitions emerge from the collective behaviour of the system. From a biological point of view and following Hopfield's arguments, the high/low activity states could be related with short term memories, so the transition between them could act as mechanisms of clearing and generating/recalling short term information. The role of the damped oscillations found in the observables' evolution is not clear yet, but it is proven to be related with transitory synchronization (Figure (2)). Since synchronization is an ubiquitous phenomenon in nature [10], and to further investigate its origin, an extension of the LA is made. A relaxation in some constraints of the model and the introduction of a new population of neurons has allowed the derivation of generalized equations (Eq. (13)). These equations are found to be in good agreement with numerical simulations and converge to the Montbrió's results [1] in the correct limit.

## ACKNOWLEDGMENTS

I would like to my advisor Alexander Roxin and co-advisor Albert Díaz-Guilera for their time and patience. I also want to show my gratitude to my family, friends and partner.

- 
- [1] E. Montbrió, D. Pazó and A. Roxin, "Macroscopic Description for Networks of Spiking Neurons", *Phys. Rev. X* 5, 021028 (2015).
  - [2] J. J. Hopfield, "Neural networks and physical systems with emergent collective computational abilities", *Proc. Natl. Acad. Sci. USA*, Vol. 79, pp. 2554-2558 (April 1982).
  - [3] A. L. Hodgkin and A. F. Huxley, "A quantitative description of membrane current and its application to conduction and excitation in nerve", *J. Physiol.* 117, 500 (1952).
  - [4] B. Gardner, I. Sporea, A. Grüning, "Encoding Spike Patterns in Multilayer Spiking Neural Networks", *arXiv:1503.09129v1 [cs.NE]* (31 Mar 2015).
  - [5] E. M. Izhikevich, "Simple Model of Spiking Neurons", *IEEE Transactions on Neural Networks*, Vol. 14, NO. 6 (November 2003).
  - [6] E. Ott and T. M. Antonsen, "Low dimensional behavior of large systems of globally coupled oscillators", *Chaos* 18, 037113 (2008).
  - [7] C. Koch, M. Rapp and I. Segev, "A Brief History of Time (Constants)", *Cerebral Cortex*, Vol. 6 NO. 2, p. 101 (1996).
  - [8] I. Ratas and K. Pyragas, "Macroscopic self-oscillations and aging transition in a network of synaptically coupled quadratic integrate-and-fire neurons", *Phys. Rev. E* 94, 032215 (2016).
  - [9] Kuramoto, Yoshiki. H. Araki, ed. Lecture Notes in Physics, "International Symposium on Mathematical Problems in Theoretical Physics", *Springer-Verlag*, 39, p. 420 (1975).
  - [10] A. Pikovsky, M. Rosenblum, J. Kurths, "Synchronization", *Cambridge University Press, Cambridge, UK*, (2001).
  - [11] \*It can be thought as a Coupling Constant in Condensed Matter Physics. It is constant due to the fully-connected scheme.
  - [12] \*\*  $\oint_{\Gamma} f(z) dz = 2\pi i \sum \text{Res}(f, a_k)$ .